Supporting Information

Osokine et al. 10.1073/pnas.1401662111

SI Materials and Methods

Isolation of Peripheral Organ and Intestinal Lymphocytes. Lymphocytes from spleen, inguinal, brachial/axillary, and mesenteric lymph nodes were isolated by mashing the organ through a 100-μm filter. For experiments in which intrahepatic or intestinal lymphocytes were analyzed, mice were perfused with 25 mL of sterile PBS by intracardiac injection to remove blood from peripheral tissues. Intrahepatic lymphocytes were isolated by mashing the respective organ through a 100-μm filter and by subsequent centrifugation in 35% (vol/vol) Percoll (GE Healthcare).

To obtain intestinal lymphocytes, the gut was first resected and flushed with D10 medium to remove digestive matter. Subsequently, the gut was divided into small and large intestine, minced, digested with DTT (1 mM in medium; Thermo Scientific), and filtered to isolate intraepithelial lymphocytes (IELs). To obtain lamina propria lymphocytes (LPLs), the undigested fraction was further digested with collagenase and DNase I (0.5 mg/mL in medium; Roche) and filtered a second time. The 40/80% (vol/vol) Percoll gradient centrifugation was used to separate IELs and LPLs from intestinal debris.

In Vivo Dendritic Cell Depletion. To deplete dendritic cells, CD11c-DTR mice were treated i.v. with 100 ng of diphtheria toxin in PBS (List Biological Laboratories) 1 d before SMARTA cell transfer. A second treatment was given 1 d after cell transfer. PBS vehicle was injected into undepleted controls.

RNA Microarray and Quantitative RT-PCR. A total of 5,000 SMARTA cells was transferred into naïve mice that were immediately infected with lymphocytic choriomeningitis virus (LCMV)-C13 (early priming) or mice infected with LCMV-Cl13 21 d earlier (late priming). Samples contained cells isolated from the spleens of six pooled mice per group. Eight days after SMARTA transfer, early- and late-primed SMARTA cells were isolated by FACSorting using an Aria II (Becton Dickinson). Postsort purity was verified as >97% on the FacsVerse (Becton Dickinson). RNA was isolated from the sorted cells using the RNeasy extraction kit (Qiagen). RNAs were evaluated using an Agilent Bioanalyzer, labeled using the Ambion WT labeling kit, and hybridized to the Affymetrix Mouse Genes ST1.0 microarrays, which were scanned and summarized using Affymetrix Expression Console and RMA16. Analysis of specific Th1 and Tfh gene products was based in part on Hale et al. (1).

For quantitative RT-PCR, RNA was prepared from sorted early- and late-primed cells, or from peripheral blood mononuclear cells. Three to four biological replicates were obtained per group. RNA was normalized for input and amplified directly using the One-Step RT-PCR kit (Qiagen). PRDM1, GRAIL, MX1, OAS, and HPRT were amplified using Applied Biosystems Assays-on-Demand TaqMan premade expression assays. mRNA amplification was detected on the iCycler (Bio-Rad Laboratories). RNA expression was normalized to HPRT.

ELISA. To quantify LCMV-specific antibodies, LCMV-M2 was used to coat 96-well Maxisorp ELISA plates (Nunc) overnight. Plates were blocked with 3% (wt/vol) BSA/PBS/0.05% Tween 20. Subsequently, serum isolated from the indicated mice was incubated on the LCMV-coated plates. Plates were washed and incubated with an HRP-labeled goat anti-mouse IgG antibody (Invitrogen), followed by the addition of *o*-phenylenediamine substrate in 0.05 M phosphate citrate buffer. The reaction was stopped with 1 M H_2SO_4, and the optical density values were read using an ELISA plate reader (Synergy 2; BioTek) at 490 nm. The concentration of antibody bound to plated virus was interpolated from a standard curve. The standard curve was generated from a serial dilution of purified mouse IgG (Invitrogen; 500–0.49 ng/mL) incubated on plates coated with goat anti-mouse IgG (Invitrogen).

KL25 Hybridoma Preparation and Neutralization Assays. KL25 B-cell hybridomas were generated by isolating $KL25^+$ B cells from TgKL25 mice. Binding of the purified KL25 antibody to LCMV-M1 and LCMV-M2 but not LCMV-Cl13 was confirmed by ELISA using plates coated with each individual virus. To determine KL25 neutralization activity against LCMV-Cl13, LCMV-M1, and LCMV-M2, each virus was individually preincubated with serial dilutions of KL25 antibody for 30 min and plaque assay performed on Vero cells. Assays were performed in triplicate.

Flow Cytometry. Analysis of immune subsets was performed by staining lymphocytes obtained from spleen, lymph nodes, liver, and intestinal fractions ex vivo for the expression of CD4, CD8, signaling lymphocytic activation molecule (SLAM), CD122 (IL-2Rβ), CD25 (IL-2Rα), CD62L, IFN-γ, TNF-α, CD138, CD11c, MHCII (I-A/I-E), CD86 (B7.2) (BioLegend); CD45.1, Granzyme B (eBioscience); and Thy1.1, B-cell lymphoma 6 (Bcl6), and Tbet (BD Biosciences). C-X-C chemokine receptor type 5 (CXCR5) expression was assessed by staining with anti–CXCR5-biotin (BD Biosciences), followed by SA-BV (BioLegend). IL-21 cytokine expression was assessed by staining with a recombinant mouse IL-21R subunit/FC chimera (R&D Systems), followed by anti–Fc-PE (Jackson Immune Research). LCMV-specific $KL25^+$ B cells were identified using antibodies against the heavy chain (clone IIIC) and idiotype (clone B2.5). Carboxyfluorescein succinimidyl ester (CFSE) dilution analysis was performed by incubating naïve SMARTA cells with 2.5 μM CFSE (Life Technologies). Flow-cytometric data were collected on the FacsVerse (Becton Dickinson).

1. Hale JS, et al. (2013) Distinct memory $CD4^+$ T cells with commitment to T follicular helper- and T helper 1-cell lineages are generated after acute viral infection. *Immunity* 38(4):805–817.

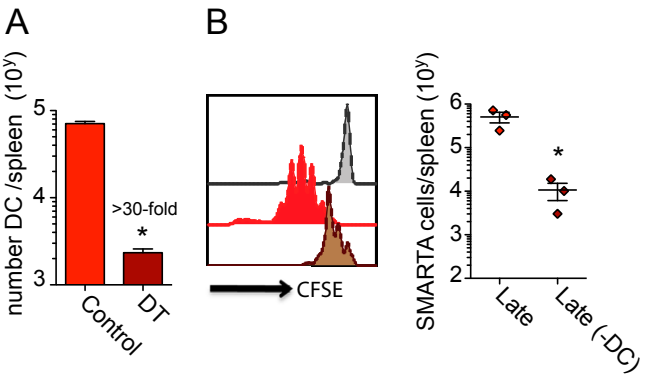

Fig. S1. Dendritic cells mediate priming during an established persistent viral infection. (*A*) On day 20 after infection, CD11c-DTR transgenic mice were treated with PBS or diphtheria toxin (DT) to deplete dendritic cells, and CFSE-labeled naïve SMARTA cells were transferred 24 h later. Twenty-four hours after transfer, mice were again given DT or PBS. Mice were killed 60 h after transfer. The graph indicates the number of $CD11c^{+}$, $MHCII^{hi}$ dendritic cells in the spleen of PBS- or DT-treated mice 36 h after final treatment. Red, PBS control; brown, DT treatment. (*B*) The flow plots demonstrate CFSE dilution and the graph indicates the number of SMARTA cells 60 h after transfer in the spleen in PBS (red)- or DT (brown)-treated mice. Gray, SMARTA cells transferred into naïve mice not subsequently infected with LCMV. $*P < 0.05$; ns, not significant. Data are representative of two independent experiments with three to four mice per group.

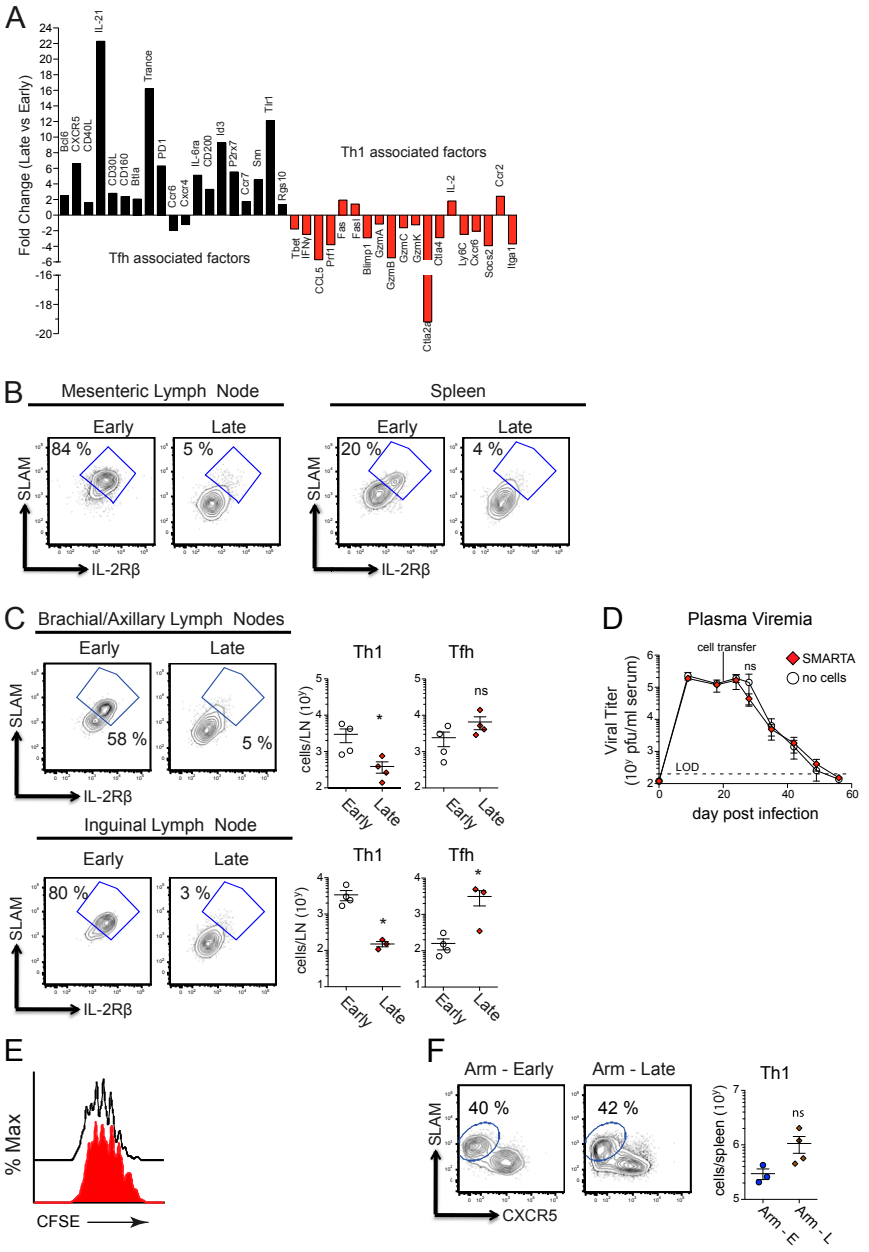

Fig. S2. Late-primed virus-specific CD4 T cells generate reduced Th1 responses within the spleen and lymph nodes and do not enhance control of viremia. (*A*) mRNA expression was compared by microarray analysis in late- vs. early-primed SMARTA cells sorted 8 d after transfer. The graph displays the relative mRNA expression, with elevated values on the *y* axis indicating increased expression in late-primed virus-specific CD4 T cells and decreased values on the *y* axis representing increased expression in early-primed SMARTA virus-specific CD4 T cells. (*B*) The flow plots illustrate Th1 (SLAM^{hi}, IL-2Rβ^{hi}) differentiation in early-primed and late-primed virus-specific T cells 8 d after priming within the mesenteric lymph nodes and the spleen. The data demonstrate the same animals from the same experiment as Fig. 2*A* to allow a direct comparison with the SLAM by CXCR5 gating strategy. (*C*) The flow plots illustrate Th1 (SLAM^{hi}, IL-2Rβ^{hi}) differentiation by virus-specific CD4^{+} SMARTA cells 8 d after early or late priming within pooled brachial/axillary lymph nodes and in the inguinal lymph nodes. The graphs indicate the number of Th1 and Tfh SMARTA cells within the organs. (*D*) Mice were infected with LCMV Cl13 and received SMARTA cells (red diamonds) or no cells (open circles) 21 d after infection. The graph illustrates plasma viral titers. LOD, limit of detection. (*E*) Mice persistently infected with LCMV-Cl13 for 21 d received either SMARTA cells or PBS control. Eight days later, CFSE-labeled SMARTA cells were transferred into both cohorts. The graph illustrates proliferation of the second round of SMARTA cells 72 h after transfer in mice that received no SMARTA cells on day 21 of infection (white open histogram), or mice that had received the first round of SMARTA cells (red filled histogram). (*F*) Naïve SMARTA cells were transferred into mice that were immediately infected with acute LCMV-Armstrong (Arm - Early) or mice that had been infected with LCMV-Armstrong 4 d previously (Arm - Late). The flow plots demonstrate Th1 formation (SLAM^{hi}, CXCR5-) in splenic SMARTA cells 8 d after transfer, and the graph shows absolute number of Th1 SMARTA cells in the spleen. *$P < 0.05$; ns, not significant. Data are representative of two independent experiments with three to four mice per group.

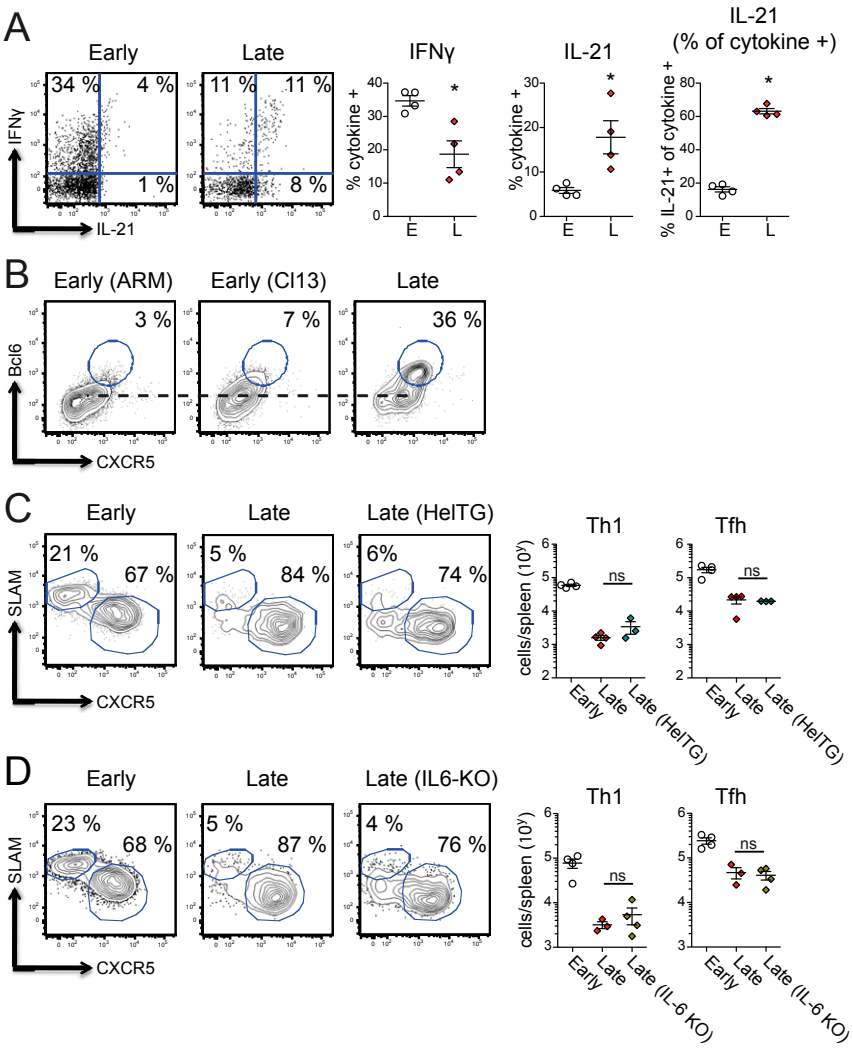

Fig. S3. Late-primed virus-specific CD4 T cells form Tfh responses without LCMV-specific B cells or IL-6. (*A*) IFN-γ and IL-21 production by SMARTA cells on day 8 after priming following ex vivo peptide stimulation. (*B*) CXCR5 and Bcl6 expression in SMARTA cells after early priming with LCMV-Arm, LCMV-Cl13, or late priming during an LCMV-Cl13 infection. The dashed line is included to facilitate a comparison of Bcl6 expression between the cohorts. (*C* and *D*) Naïve SMARTA cells were transferred 21 d after LCMV-Cl13 infection into C57BL/6 WT or (*C*) B-cell transgenic mice encoding an antibody specific to hen egg lysozyme (Hel-tg) that have B cells, but do not express anti–LCMV-specific B cells, or (*D*) IL-$6^{-/-}$ mice. The flow plots illustrate Th1 ($SLAM^{hi}$, $CXCR5^{-}$) and Tfh ($SLAM^{lo}$, $CXCR5^{+}$) differentiation by virus-specific CD4 SMARTA T cells in the spleen 8 d after priming. The graphs represent the absolute number of Tfh and Th1 SMARTA cells. *$P < 0.05$; ns, not significant. Data are representative of two to four independent experiments with three to five mice per group.

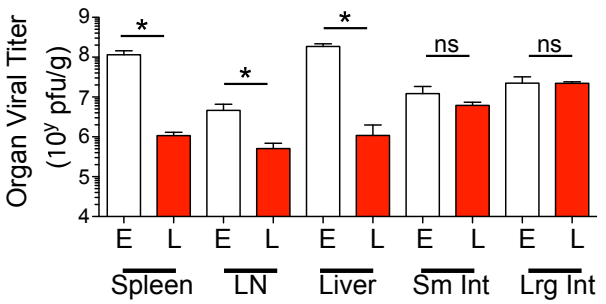

Fig. S4. Viral titers within lymphoid and peripheral organs early and late after infection. Viral titers (plaque-forming units per gram tissue) in spleen, inguinal lymph nodes, liver, and small and large intestine on day 8 and day 29 after infection. The times represent the equivalent of 8 d after early or late priming. Data are representative of two independent experiments with four mice per group.

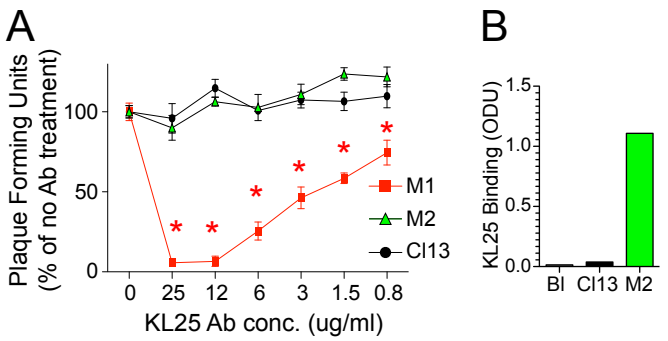

Fig. S5. Binding and neutralization of LCMV-isolates by KL25 antibody. (*A*) Neutralization of LCMV-Cl13 (black), LCMV-M1 (red), and LCMV-M2 (green) by the KL25 antibody. The graphs demonstrate the number of viral plaques as a percentage of no antibody control. (*B*) A fixed concentration of KL25 antibody was coincubated with media alone (blank), with 2×10^6 plaque-forming units of LCMV-C13, or with 2×10^6 plaque-forming units of LCMV-M2. Antibody binding was determined by ELISA and is displayed as optical density units (ODU). $*P < 0.05$. Data are representative of two independent experiments.

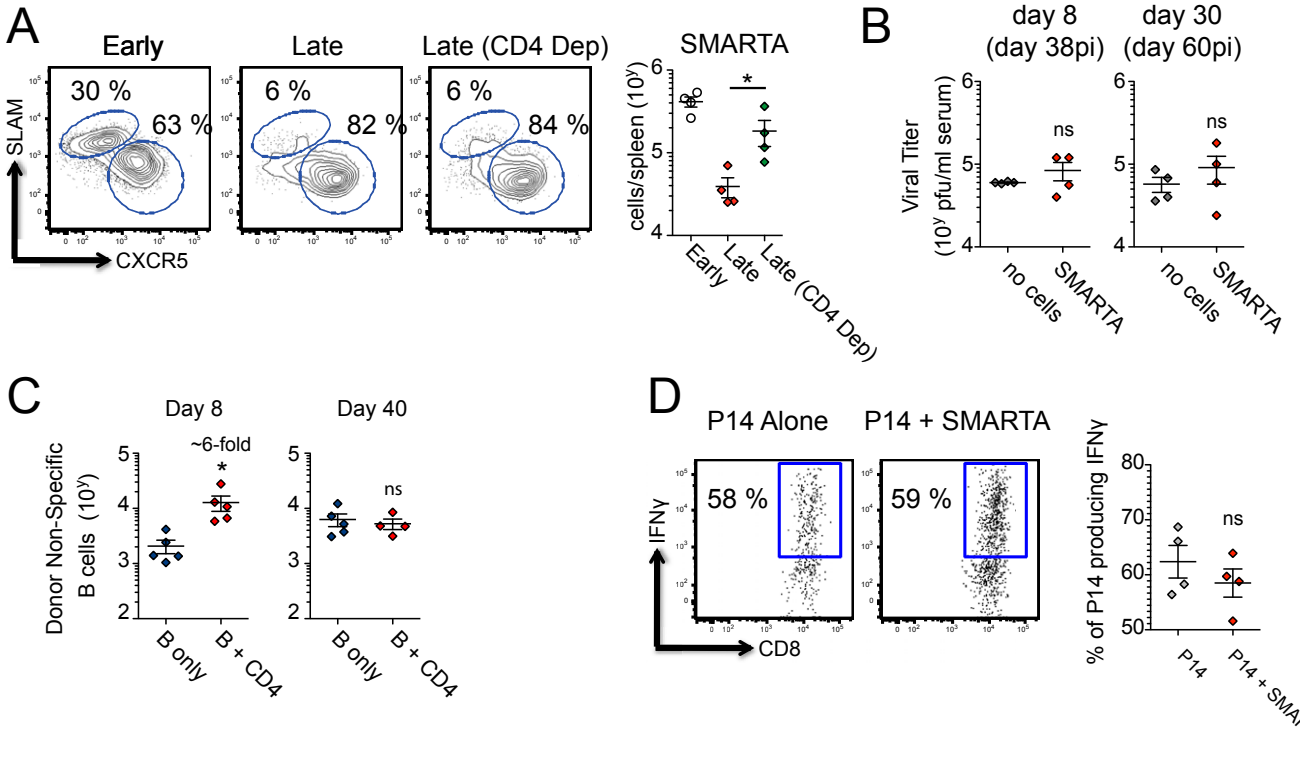

Fig. S6. Preexisting antiviral CD4 T-cell responses do not affect the late-primed Th1 defect, and the late-primed CD4 T cells do not provide enhanced help to non–LCMV-specific B cells or LCMV-specific T cells. (*A*) Th1 and Tfh generation in early- and late-primed cohorts and in a cohort of mice that were CD4 depleted before infection with LCMV-Cl13 and received SMARTA cells 30 d after infection. The flow plots and graphs illustrate the percentage of Th1 and Tfh SMARTA cells and the number of SMARTA cells within the spleen 8 d after transfer. (*B*) Mice were CD4 depleted before LCMV infection. Thirty days after infection, mice received either SMARTA cells or no cells, and plasma virus titers were quantified on days 8 and 30 after transfer (38 and 60 d after infection). (*C*) Non–LCMV-specific, splenic donor B cells from TgKL25 mice (i.e., heavy chain positive, anti-idiotype antibody staining negative) were quantified numerically on days 8 and 40 after cell transfer. (*D*) The flow plots and graph illustrate IFN-γ^+ secretion by virus-specific P14 cells 8 d after transfer alone or with SMARTA cells. Transfer was performed into persistently infected mice that were CD4 depleted before infection. $*P < 0.05$; ns, not significant. Data are representative of four independent experiments with three to four mice per group.

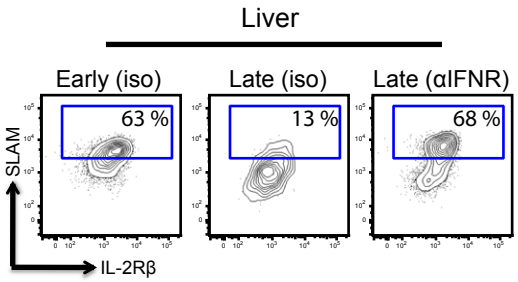

Fig. S7. IFNR blockade restores Th1 formation within the liver. The flow plots illustrate Th1 (SLAM^{hi}, IL-2Rβ^{hi}) formation in liver SMARTA cells 8 d after early or late priming and isotype treatment (iso) or anti-INFR blocking antibody treatment. Data are representative of four independent experiments with three to four mice per group.

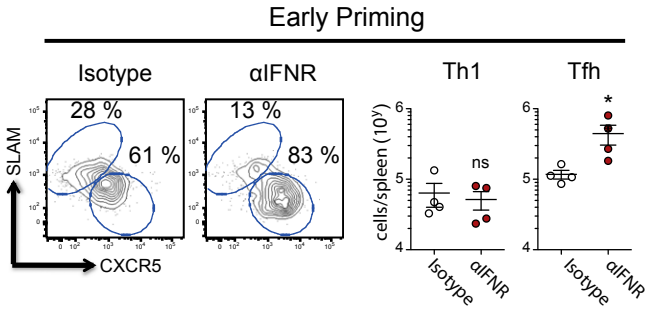

Fig. S8. IFNR blockade at the onset of persistent infection leads to enhanced Tfh but not Th1 formation. The flow plots and graphs illustrate Th1 and Tfh formation by splenic SMARTA cells 9 d after isotype or anti-IFNR blocking antibody treatment at the onset of infection. *$P < 0.05$; ns, not significant. Data are representative of four independent experiments with three to four mice per group.

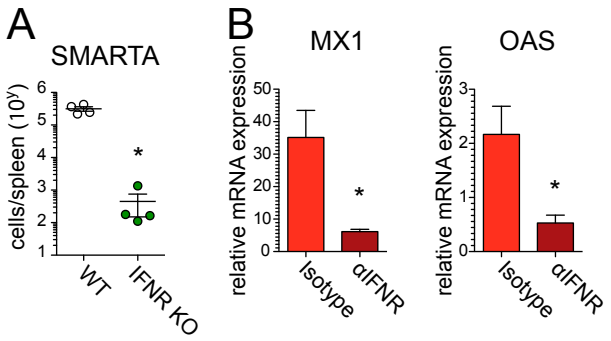

Fig. S9. IFN-I signaling during is required for early-primed virus-specific CD4 T-cell survival, and anti-IFNR blockade suppresses IFN-I signaling within 24 h of treatment. (*A*) WT or IFNR$^{-/-}$ SMARTA cells were transferred into mice immediately before LCMV-Cl13 infection. The graph shows the number of splenic SMARTA cells 8 d after infection. (*B*) On day 21 after LCMV-Cl13 infection, mice were treated with isotype or anti-IFNR blocking antibody. The graphs display mRNA expression of IFN-inducible genes MX1 and OAS in peripheral blood mononuclear cells 24 h after treatment. *$P < 0.05$. Data are representative of two independent experiments with four mice per group.